CERN-ACC-NOTE-2020-0031

24 May 2020
emilia.cruz-alaniz@cern.ch

RF multipoles deliverable

E. Cruz-Alaniz[1], Y. Papaphilippou[2], C. Welsch[1]
[1]University of Liverpool and the Cockroft Institute, UK, [2]CERN, Switzerland

Keywords: Crab Cavities, HL-LHC, higher order multipoles, Dynamic Aperture

The crab cavities to be installed in the High-Luminosity LHC (HL-LHC) aim to provide an increase in luminosity by restoring head-on collisions and therefore reducing the loss of luminosity due to the crossing angle. The crab cavities rotate the beam by providing z-dependent kicks near the interaction point. Two designs have been cast for this task: the RF dipole (RFD) and the Double Quarter Wave (DQW); a prototype of the latter one has been installed in the SPS and in 2018 the first successful crabbing of proton beams was achieved. As the design of both these crab cavities has to be very compact to be able to fit between the two beams, this causes a loss of axial symmetry that gives rise to high order multipoles. This study aims to explore the impact and tolerances of the high order multipoles on beam dynamics by performing DA studies on the HL-LHC lattice.

Contents

1 Introduction and motivation

The lack of azimuthal symmetry for the compact design of the crab cavities to be able to fit between the two proton beams, higher order multipoles (named RF multipoles) are present inside the cavities. These RF multipoles are expected to have an impact on beam dynamics which can be studied via long term tracking. Dynamic Aperture (DA) studies have been previously done using an earlier version of the crab cavity model (4ROD) [1]; this study also explored the tolerances of each multipole by increasing each one of them individually and observing its impact on DA. The only component with a significant impact on DA was the quadrupolar (b_2) component, while the sextupolar (using skew sextupolar a_3 due to vertical crossing) and octupolar (b_4) components did not show any significant impact on DA, even when increasing them to very large values. Complementary studies recommended the reduction of the sextupolar component to less than 1000 mT/m to relax the orbit misalignment to 1 mm and the recommendation for the higher order values to be below 10^n [2], when n indicates the order of the RF multipole.

Several design changes have been done since these previous studies: the crab cavity designs have now converged to the DQW design (providing deflection in the vertical plane) [3] for Interaction Region 5 (IR5) and the RFD (providing deflection in the horizontal plane) [4] for Interaction Region 1 (IR1); the crossing plane has changed to horizontal in IR1 and vertical in IR5 and the crossing angle was reduced from 590 μrad to 500 μrad; and finally, a series of changes from the HLLCV1.1 (used for previous studies [1]) lattice version, to the one used for these studies (HLLHCV1.3 [5]). Two crab cavities per beam and per IP side for a total voltage of 6.8 MV are assumed in the following simulation. The following sections explain the calculation of RF multipoles for the latest designs of crab cavities, their implementation on the HL-LHC lattice, and finally DA studies to observe their impact.

2 RF multipole measurements

The RF multipoles can be treated in a similar way as the magnetic multipoles in the sense that the total field can be decomposed into an infinite sum of multipoles, such that:

$$B_y + iB_x = B_{ref} \sum_{n_1}^{N} (b_n(r_0) + ia_n(r_0)) \left(\frac{x+iy}{r_0}\right)^{n-1}, \tag{1}$$

where $B_{x,y}$ refer to the magnetic field in the horizontal and vertical direction, and b_n and a_n the normal and skew components respectively. But, contrary to the magnetic multipoles, the RF multipoles are oscillating at the crab cavity frequency of 400 MHz and the kick depends on the longitudinal position. The RF multipoles are therefore given as complex numbers [6]; the real part representing the case when the particle at $z = 0$ has the maximum deflection, while the imaginary part represents the case when the particle at $z = 0$ (with respect to the synchronouse particle) sees no kick.

One can obtain the multipole coefficients b_n and a_n by different ways. This work uses the coefficients calculated with two methods. The Lorentz-Force (LF) calculates the coefficients via the force [1]:

$$a_n = \frac{1}{qc}\frac{1}{\pi}\int_{-\pi}^{\pi}\frac{1}{\rho^{n-1}}\sin(n\phi)\int_0^L F_\rho(\rho,\phi,s)dsd\phi, \tag{2}$$

$$b_n = \frac{1}{qc}\frac{1}{\pi}\int_{-\pi}^{\pi}\frac{1}{\rho^{n-1}}\cos(n\phi)\int_0^L F_\rho(\rho,\phi,s)dsd\phi; \tag{3}$$

where ρ, ϕ and s are the cylindrical coordinates. The Panowski-Wenzel (PW) method, calculates them via the electric field [1]:

$$a_n = \frac{in}{\omega}\frac{1}{\pi}\int_{-\pi}^{\pi}\frac{1}{\rho^{n}}\sin(n\phi)\int_0^L e^{\frac{i\omega}{c}s}E_s(\rho,\phi,s)dsd\phi, \tag{4}$$

$$b_n = \frac{in}{\omega}\frac{1}{\pi}\int_{-\pi}^{\pi}\frac{1}{\rho^{n}}\cos(n\phi)\int_0^L e^{\frac{i\omega}{c}s}E_s(\rho,\phi,s)dsd\phi. \tag{5}$$

Discrepancies can be observed between the two methods due to details on the mesh. The LF method might be a more reliable approach since it converged faster with the number of azimuthal points used than the PW method [7], but for this study the PW method was chosen as it provides the largest values, and therefore corresponds the worst case scenario.

The latest values for the quadrupolar, sextupolar and the octupolar components of the DQW and RFD that are used for this work are given in Table 1 [8].

	Panofzky-Wenzel method (PW)					
	b_2		b_3		b_4	
	Re	Im	Re	Im	Re	Im
LHC DQW	6	-3	1506	27	2016	-539
LHC RFD	0	0	-522	-56	-914	-36
	Lorentz Force method (LF)					
	b_2		b_3		b_4	
	Re	Im	Re	Im	Re	Im
LHC DQW	6	-2	1488	21	1048	-292
LHC RFD	0	0	-458	-74	128	55

Table 1: RF multipoles (in units of $\mathrm{mTm/m}^{n-1}$) measured via the PW and the LF method for the DQW and RFD crab cavity models normalized to a RF voltage of 10 MV.

From the numbers it is noticeable that the real part of the quadrupole component (b_2) has significantly increased from the 4ROD version used for the previous studies (from -0.06 mT to 6 mT) for the DQW, while for the RF dipole this component is not present. The sextupolar component is slightly larger than the one used previously for the DQW (1506 versus 1159 mT/m) but lower, and with different sign, for the RFD (-522 mT/m). For the octupolar component there is also an increase of about 2 orders of magnitude, from -4 mT/m^2 present in the 4ROD, to 2016 mT/m^2 for the DQW and to -914 mT/m^2 for the RFD.

This work aims to build on the previous studies, implementing the updated values in the new lattice and run DA simulations. Among the things to be checked are whether the increase in the quadrupolar and octupolar components, with respect to the last version, will have an effect on the DA; also, for the sextupolar component, whether the change in sign between the two models influences the stability. Studies will also include beam-beam effects, which have not been simulated before in combination with RF multipoles; and finally, the implementation of misalignments to ensure that the system is able to tolerate a misalignment of up to 1 mm in crab cavities without loss of DA.

3 Implementation

The RF multipoles were implemented into the HLLHCV1.3 version of the HL-LHC lattice ([5]) using the code MADX [9] which has a class dedicated to these elements. For horizontal crossing (RFD) the quadrupolar, sextupolar and octupolar components are implemented in MADX as $\{K_{N,1}L, K_{N,2}L, K_{N,3}L\}$, where $K_{N,n}L$ are the integrated strengths of the multipolar components in units of $[\mathrm{m}^{-n}]$, given in terms of b_{n+1} as [6]:

$$K_{N,n}L = n!\frac{b_{n+1}}{B\rho} \tag{6}$$

where $B\rho$ is the beam rigidity. For the vertical crabbing, due to the 90° rotation, these values are instead implemented as $\{-K_{N,1}, K_{S,2}, K_{N,3}\}$. The skew sextupolar component is defined equivalently to the normal multipoles as:

$$K_{S,n}L = n!\frac{a_{n+1}}{B\rho} \tag{7}$$

It is also important to notice that when implementing the corresponding RF multipoles into MADX they need to be adjusted to the corresponding CC voltage. In this case the RF multipoles from Table 1 were normalized to 10 MV, but the CC voltage in HL-LHC was 3.4 MV per CC. The values from Table 1 were therefore multiplied by 0.34 when there were implemented in MADX.

DA studies were performed using SixTrack [10] with 10^6 turns, 5 angles, 60 seeds, no beam-beam, and 6D tracking. All simulations in this work were also done with a complete set of errors, including errors in the arcs, inner triplet and separation and recombination dipoles. The half crab crossing was set to 190 μrad and the nominal half crossing angle for the HL-LHC is 250 μrad; the studies presented here however, were done with an earlier value for half crossing angle of 255 μrad. DA studies were done for the nominal case including RF multipoles and 250 μrad crossing angle for comparison and no significant differences on DA were observed. The same is expected in the rest of the studies.

Figure 1 shows the comparison between the case when the crab cavity voltages are set to zero (in blue); then, when the integrated voltage at either side of IR1 and IR5 is set to 6.8 MV, but without RF multipoles (in red); and finally, the case when RF multipoles (given in Table 1 with the PW model) are implemented for different crossing scenarios: horizontal crossing in IR1 and vertical crossing in IR5 (hv) in blue, and vertical crossing in IR1 and vertical crossing in IR5 (vh) in black. All future studies in this work will be done with the current baseline crossing for HL-LHC (hv).

As can be seen from the results, a small effect can be observed by the implementation of either the crab cavity voltage or the RF multipoles, but the overall minimum DA, dictated by the lowest angle (15°) stayed the same for all cases.

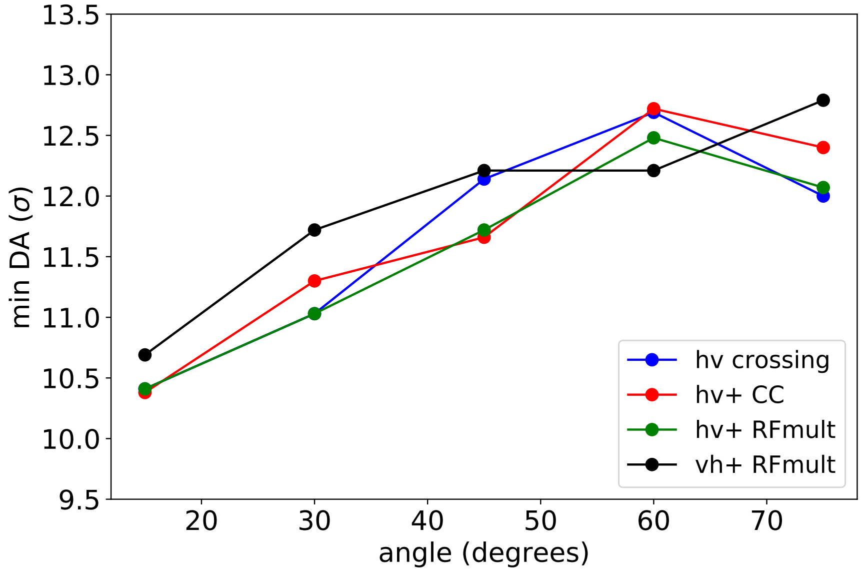

Figure 1: Minimum DA vs angle, with cavities with voltage set to 0 MV and hv crossing (blue), with voltage on 3.4 MV per cavity (red) and with RF multipoles on the crab cavities with hv (green) and vh (black) crossing.

The following sections focus in each individual component to study the limit before the DA starts getting affected, also for the cases when misalignments or beam-beam effects are included. The motivation of this study is to understand how far are the designs from the limit, and to estimate how much we can tolerate in case the crab cavity designs, and therefore the RF multipoles, change in the future.

3.1 Quadrupolar component

As seen in Table 1, the quadrupolar component for the DQW was estimated to 6 mT, while it was zero for the RFD. The value for b_2 in DQW was scanned and the DA was calculated for each case, while the other multipoles were kept unchanged, including the b_2 set to zero in the RFD. Figure 2 shows the DA vs b_2 values. From the figure the effect on the DA of the increasing quadrupolar component in DQW is noticeable, but the effect is only significant until b2 is increased to around 30 mT, or 5 times the nominal value, when a decrease is observed in all angles. The expected linear tune shift for a normal quadrupolar component is given as [11]:

$$Q_{\text{shift}} = \frac{1}{4\pi}\beta_{x,y}\frac{b_2}{B\rho}, \tag{8}$$

so, with the β function at the location of the crab cavities oscillating between 3000 and 4000 m, the expected linear tune shift per CC for a b_2 of 30 mT is of the order of $Q_{\text{shift}} = 3 - 4 \times 10^{-4}$.

To study the effect of possible misalignments, a 1 mm deviation of the position of the crab cavities, and therefore the RF multipoles, was added on cavities left and right on both interaction regions. This misalignment corresponds to moving both cavities left and right of the IP to the same direction, and on the plane of the corresponding crossing (horizontal on

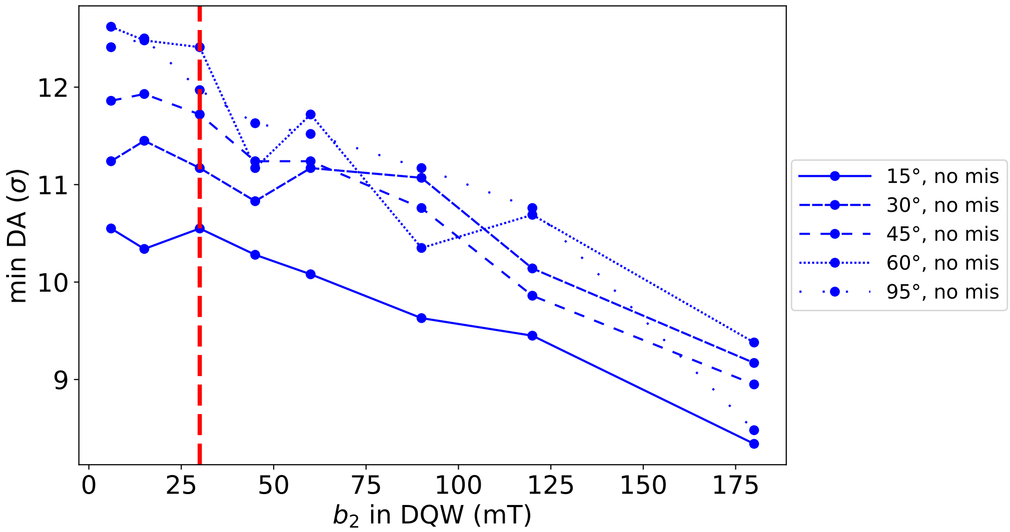

Figure 2: Minimum DA for 5 angles with increasing b_2 component on the DQW crab cavity in IR1. The rest of the RF multipoles were kept at the nominal values. No misalignments or beam-beam effects are considered in this case. The limit at which the DA starts to get significantly reduced is also indicated in the figure (red line).

IR1 and vertical on IR5). The results for all 5 angles are shown in Fig. 3. As can be seen from the figure, the misalignment had little to no effect and the overall minimum DA, and therefore the limit, remained the same for both cases.

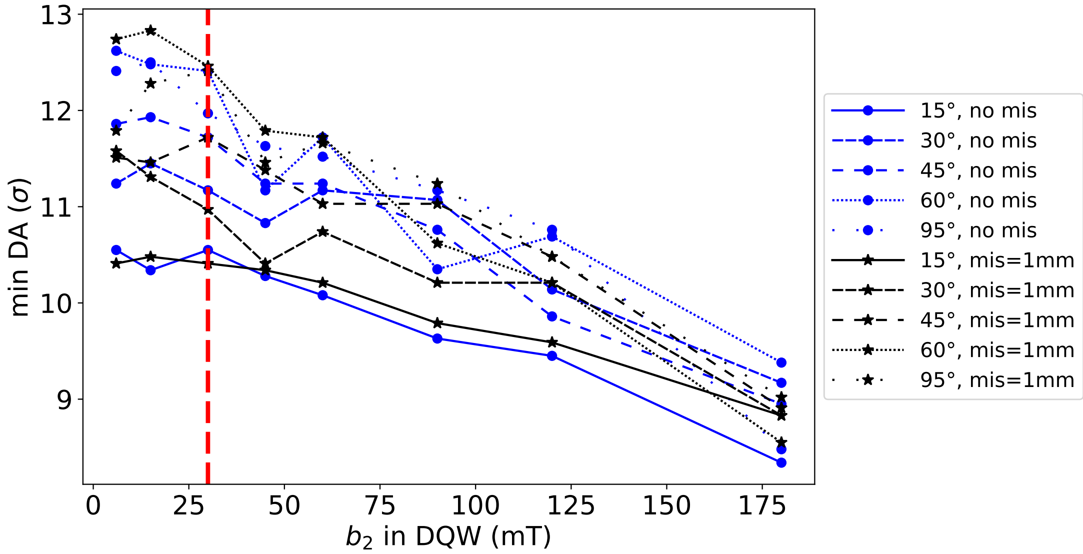

Figure 3: DA for 5 angles angles with increasing b_2 component on the DQW crab cavity in IR1 with crab cavities on and without misalignments (blue), and when a misalignment of 1 mm is added (black). The limit at which the DA starts to get significantly reduced is also indicated in the figure (red line).

Now, misalignments are not considered but beam-beam effects were added to the simulation. After optimizing the working point for this case, the results are shown in Fig. 4. Results show that for this case the limit is slightly higher than for the case without beam-beam, with no significant reduction for this case until b2 increases to 90 mT (around 15 times the nominal value). This is possibly explained by the fact that the beam-beam effects dominate the losses, and the effect of RF multipoles becomes noticeable only for higher values. Using Eq. 8, we can calculate that 90 mT per CC is equivalent of a tune shift of $Q_{\text{shift}} \sim 10^{-3}$.

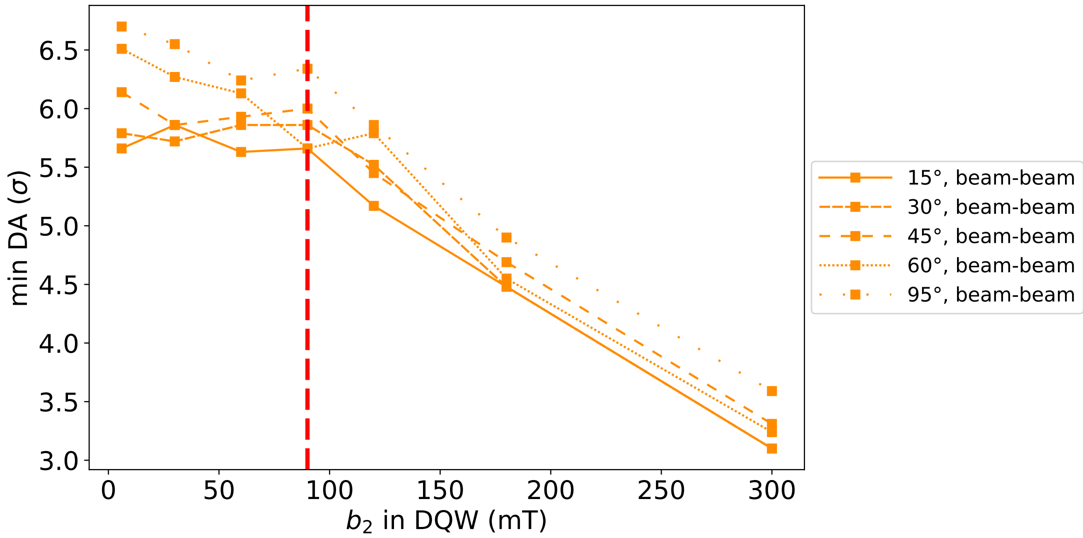

Figure 4: DA for 5 angles for increasing quadrupolar component and 1 mm misalignments in the DQW and the RFD crab cavities in IR1 and IR5. Beam-beam effects are also considered. The limit at which the DA starts to get significantly reduced is also indicated in the figure (red line).

As said previously, a quadrupolar component was implemented only in the DQW crab cavity model, but was set to zero on the RFD. Studies were also performed implementing this component also in the RFD, to observe how the adding up or mitigation of this component between the two main interaction regions change the limits on stability. From the results shown in Fig. 5 it is clear that the limits on DA variation depend on the sign between multipoles of both crab cavity models. Note that when the b_2 multipoles have the same design sign (effectively corresponding to having opposite values of the b2 errors in the DQW and RFD cavities due to the different crabbing plane in IP1 and IP5) is pessimistic. The impact on DA becomes significant at 30 mT, the same value than the case without quadrupolar component on RFD, but for this case the DA decays much faster for higher values of b_2. On the contrary, when the quadrupole multipoles (b_2) have the opposite design sign, the two components cancel out resulting in a more stable scenario, with the limit at 60 mT (or 10 times the nominal value); this latter scenario is therefore even better than the case where no quadrupole components are present in IR1. Although the present quadrupole components in the CCs are currently far away from the limit, this last result is important to take into account in case these values increase or a quadrupole component is present in the crab cavities at both IRs, such as using the same DQW model for both IRs for example.

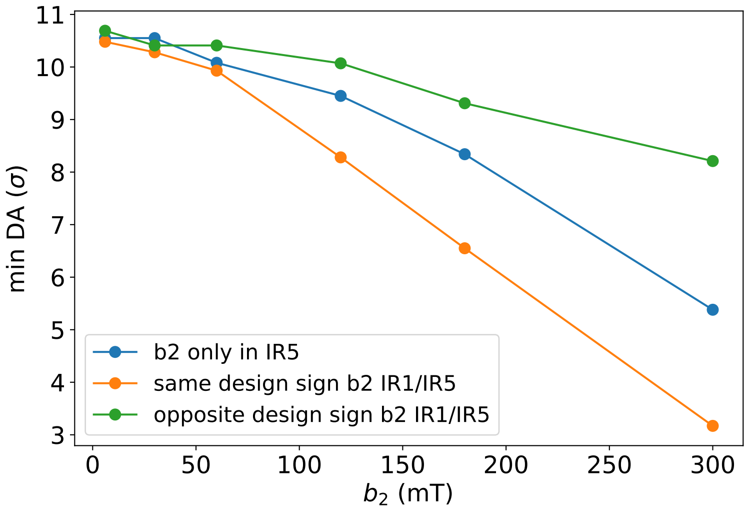

Figure 5: Minimum DA for 5 angles with increasing quadrupolar component only in IR5 (blue); and when including quadrupolar component also in the IR1 with the same (orange) and opposite (green) sign than in IR5.

3.2 Sextupolar component

DA studies were now repeated by increasing the sextupolar component in both cavities. For the sextupolar component we have contributions in both the RFD and DQW models, implemented as normal (b_3) and skew (a_3) sextupole, as explained in Sec. 3. There is also a difference in value and sign between both models (-522 mT/m and 1506 mT/m in RFD and DQW respectively).

Figure 6 illustrates the DA vs the scale factor of the nominal sextupole contribution (different between RFD and DQW) for cases without misalignments, and when 1 mm misalignment is added. Results show that the first case is very stable, even for very large values of sextupolar contributions; however, when 1 mm misalignment is added the limit is met much sooner. Figure 7 shows the case with 1 mm misalignment only, to better observe the tolerances. As can be seen from the figure, the limit can be drawn at around 20 times the nominal value of the sextupolar component ($\sim$10 $\times 10^3$ mT/m), where a significant reduction of DA is observed at all angles.

The misalignments assigned for these cases correspond to moving all cavities left and right of each IR to the same direction of the corresponding crossing plane (both positive horizontal misalignments for IR1 and both positive vertical misalignments for IR5). To make sure this is the worst case scenario simulations were done in the zone where the reduction of DA is observed, that is between 20 and 40 times the nominal values. Results are shown in Fig. 8. The specifications to what each misalignment case refers to is given in Table 2. As can be seen from the figure this region of units of sextupolar component observes a reduction of DA for the cases where all cavities left and right of both IRs were moved to the same direction (positive positive or negative negative) of the corresponding crossing plane; but such reduction is not observed on the other two cases when left and right CCs were moved on opposite directions (positive misalignments in left CCs and negative misalignments in right CC's and vice versa). Therefore, the first two cases were consider the worst case

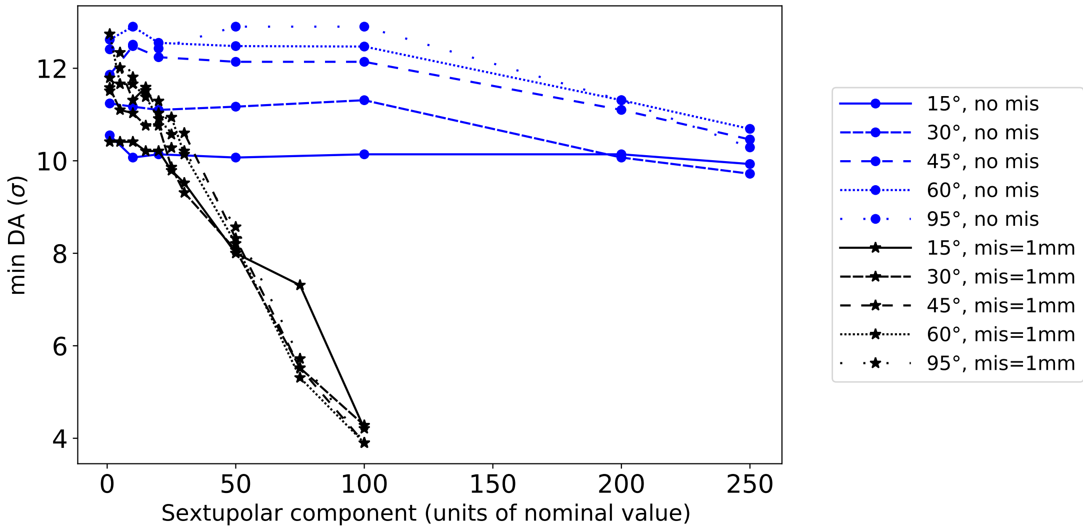

Figure 6: Minimum DA for 5 angles with increasing sextupolar component on both DQW and RFD crab cavities. Cases without misalignments (blue), and when a misalignment of 1 mm is added (black) are shown

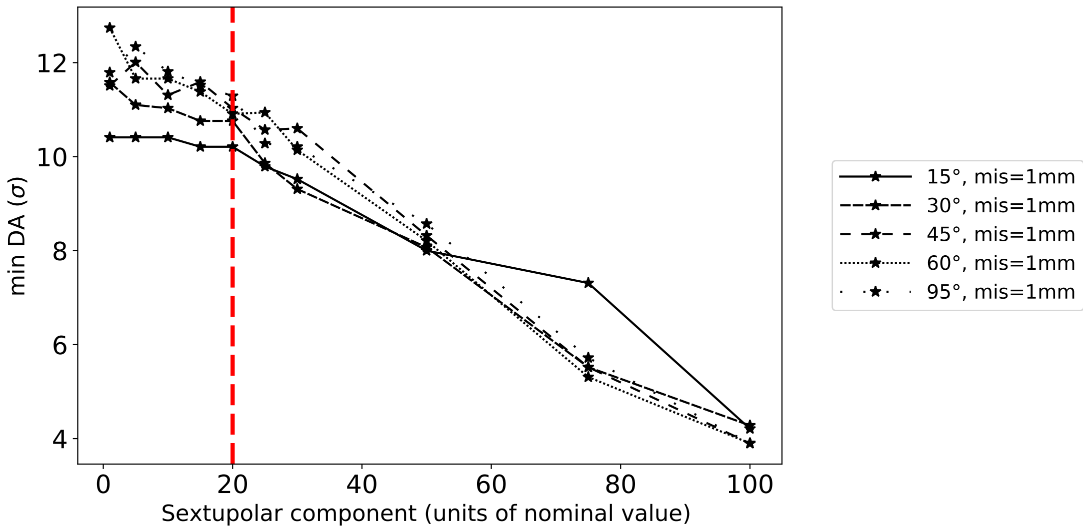

Figure 7: DA for 5 angles for increasing sextupolar component and 1 mm misalignments in the DQW and the RFD crab cavities in IR1 and IR5. The limit at which the DA starts to get significantly reduced is also indicated in the figure (red line).

scenarios. For all further studies when misalignment are considered the positive positive case is the one taken into account.

The same studies were repeated now including beam-beam effects and results are shown in Fig. 9. The tolerances for this component are the same as for the case without beam-beam effects, with the limit found at 20 times the nominal values.

Finally for this case in order to explore the effect of the difference in sign between sextupolar components in both CC models, we changed the sextupolar contribution from RFD

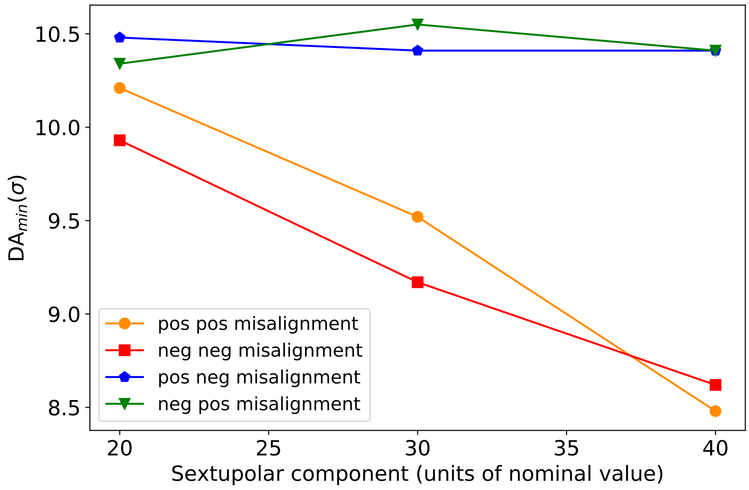

Figure 8: Minimum DA for 5 angles with increasing sextupolar component on both DQW and RFD crab cavities. Four cases of different misalignments are presented. The first two refer to the case where all cavities are misaligned to the same direction of the corresponding crossing plane (horizontal in IR1 and vertical in IR5) with both positive (orange) and negative (red) misalignments. The other two refer to the case when the cavities left and right of the IP are misaligned to opposite directions of the corresponding crossing plane, for both positive misalignments in the left CCs and negative on the right (blue) and vice versa (green). More details on the direction of the misalignments are given on Table 2.

Table 2: Summary table of the direction of misalignment cases presented in Fig. 8.

Name	**Left CCs IP1**	**Right CCs IP1**	**Left CCs IP5**	**Right CCs IP5**
pos-pos misalignment	positive in x	positive in x	positive in y	positive in y
neg-neg misalignment	negative in x	negative in x	negative in y	negative in y
pos-neg misalignment	positive in x	negative in x	positive in y	negative in y
neg-pos misalignment	negative in x	positive in x	negative in y	positive in y

to positive values (changed from -522 mT/m to 522 mT/m) and increased it by the same amount as we did for the case with 1 mm misalignments in Fig. 7. The sign of all the other multipolar components remained the same as in Table 1. The comparison between both cases is shown in Fig. 10 in which we observe the importance of the sign: the case with same sign between both models is much more stable, where the limit can be drawn at around 30 times the nominal value, to compare with the 20 times for the negative sign on the sextupolar component in the RFD. This last result shows the importance of the sign between the models and could even provide a method of mitigation if the limit is reached, although currently we are by far safe from that limit and such mitigation is not necessary.

We now used both cases presented in Fig. 10 and compare it with the results obtained in Fig. 2 to calculate the feedown from the sextupole effects with misalignments in quadrupole terms. For this, the DA was plotted vs the sum of the absolute values of b_3 and a_3, and then a calculation was made to which n the graph DA vs $n * b_2$ was equivalent. Results in Fig. 11 show that n=500 shows really good agreement with DA vs $|b_3| + |a_3|$ for the case when b_3

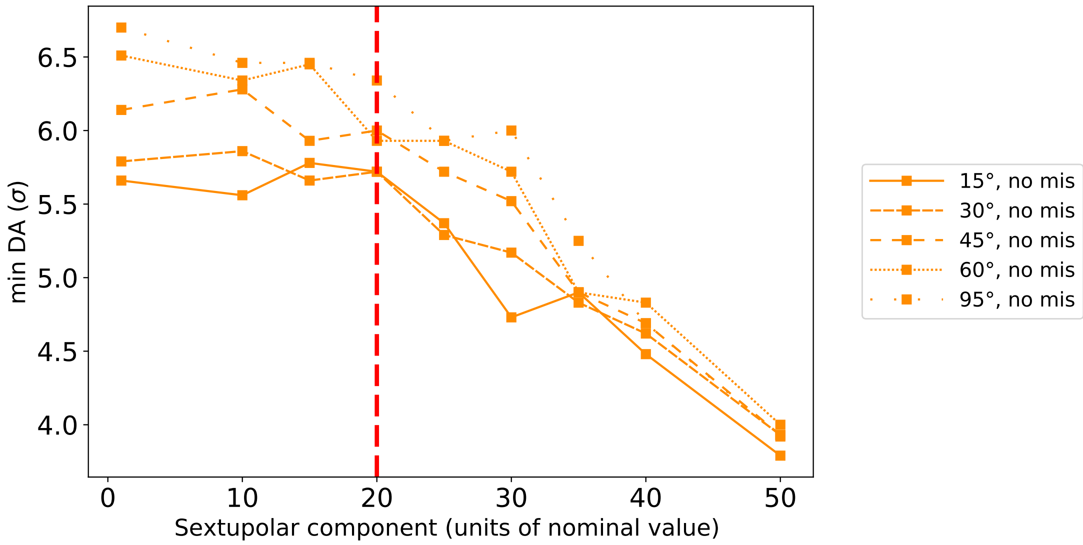

Figure 9: DA for 5 angles for increasing b_3 component and 1 mm misalignments in the DQW and the RFD crab cavities in IR1 and IR5. Beam-beam effects are also considered. The limit at which the DA starts to get significantly reduced is also indicated in the figure (red line).

is negative in RFD (black line in Fig. 10), that means that for this case 1 unit of b_3 with 1 mm misalignment is equivalent to 500 units of b_2. For the case when b_3 in RFD is positive (green line in Fig. 10) n increased to 1000.

3.3 Octupolar and higher order components

Studies were repeated increasing higher order multipoles like the octupolar or the decapolar component. For the octupolar component the nominal values from the PW model in Table 1 were taken, with 2016 mT/m^2 for DQW and -914 mT/m^2 for the RFD. The octupolar component was increased up to very large values (around 200 times the original values) but no impact was observed in any of the cases: no misalignments, 1 mm misalignment, or when including beam-beam effects.

For decapolar components no values were given in the results in Table 1. Values were estimated from the RFD design discussed in [4] which was calculated to be 2.0×10^5 mT/m^3 for 1 MV. This value is above the limit of 10^n mentioned in the introduction for higher orders (10^5 for this case) and therefore studies were done to estimate the tolerances; however, no impact was observed on DA, even when increasing this component up to 100 times the nominal value.

3.4 Imbalance between CC parameters

To study the effect on DA of the proton bunch failing to close perfectly locally, a study was done in which the phase of the CC's on the right hand side (where the closing takes place) is shifted by a certain amount. No beam-beam effects or misalignments were considered for this study. The result is illustrated in Fig. 12. As seen from the figure the effect of the

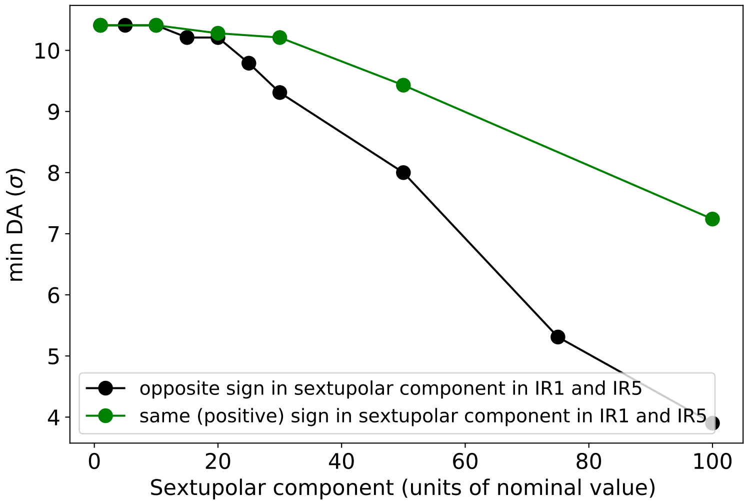

Figure 10: DA for 5 angles with increasing b_3 component when 1 mm misalignment on the CC and RF multipoles for the nominal values: positive values in IR5 and negative values in IR1 (black), and for the case with positive values in both IR5 and IR1.

phase on DA is noticeable along all 5 different angles and overall minimum DA. As it can be seen from the figure, a change of 45 degrees can have significant effects on DA. Further studies could be made to analyze the effect on a shorter range ($\pm 10°$), more likely to occur when considering a phase error, and for further scenarios: different phase shifts for both IPs, including beam-beam effects, etc.

A further test was done to check how the DA was impacted when an imbalance exists between the voltage in the crab cavities at either side of the IPs. DA studies were done for different values of b_2, as it was presented in Fig. 2, but for this case the value of the voltages on the right hand side CC's of both IPs, and hence their RF multipoles, were taken to be 20% higher than those on the left CC's. The results are presented in Fig. 13. As shown in the figure, no difference is observed between the cases with same voltage at either side and those with an imbalance on the right side for lower values of b_2, but for b_2 larger than 100 mT a left/right imbalance of the voltage of the crab cavities can result in a further reduction of the DA.

4 Conclusions

The crab cavities to be installed in the HL-LHC promise an increase in luminosity by recovering the geometrical reduction due to the crossing angle. However, compromises have been done to the field quality in order to have these cavities fitted between the two beams; this study measured the tolerances to different orders of multipolar kicks to make sure this loss of field quality will not affect the beam dynamics enough to be detrimental to the DA.

The multipolar kicks were measured for both models of crab cavities: the RFD for the horizontal crossing, and the DQW for the vertical one. After implementing these multipolar components in the lattice, DA studies were performed to analyze whether an impact is observed. Results show that for the nominal case, with the measured values in both the RFD

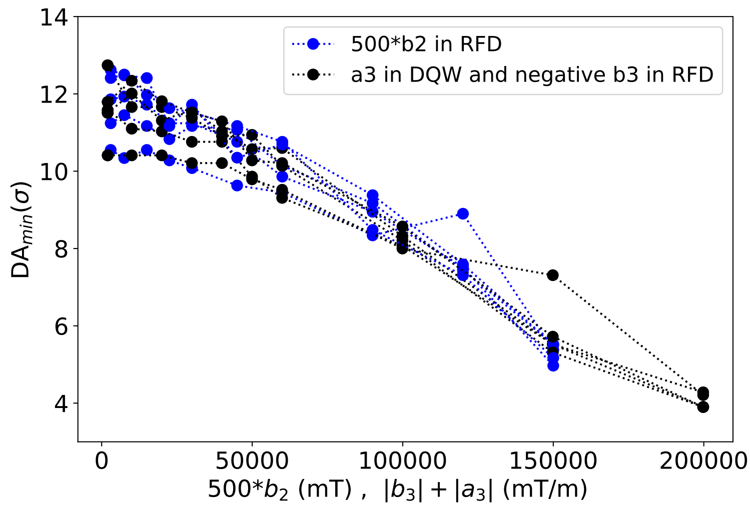

(a)

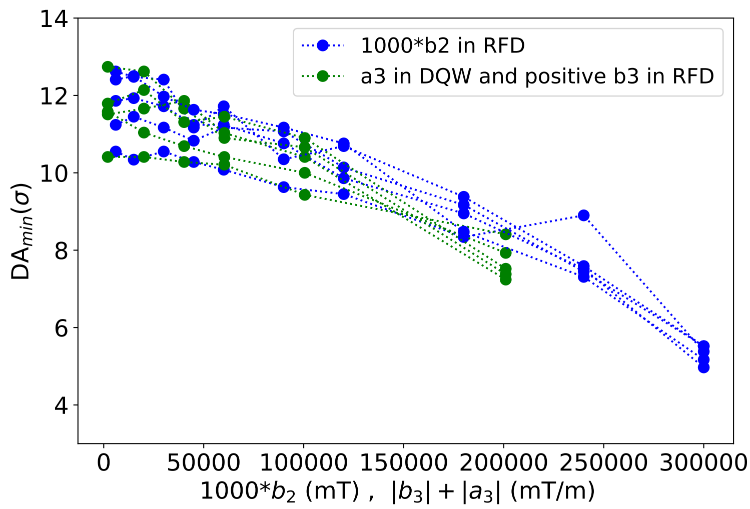

(b)

Figure 11: Comparison of DA vs the sum of the absolute units of b_3 and a_3, and DA vs n*b_2, where n was calculated when a good agreement was found between the two graphs. Two cases are presented: (a) when b_3 in RFD has a negative sign which results in 1 unit of sextupole and 1 mm misalignment equivalent to 500 units of b_2 and (b) when b_3 in RFD has a positive sign, which results in 1 unit of sextupole and 1 mm misalignment equivalent to 1000 units of b_2. In both cases a_3 in DQW is positive.

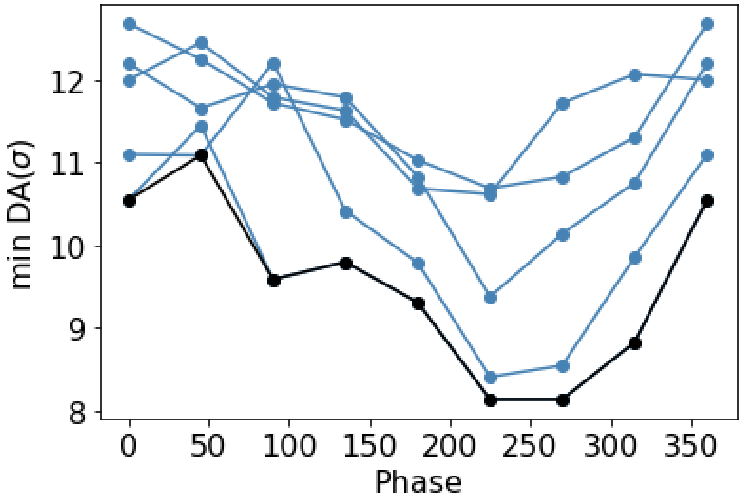

Figure 12: Minimum DA for 5 different angles (DA) as a function of the change in phase of the crab cavities in the right side of IP1. The minimum DA of all 5 angles is shown in black.

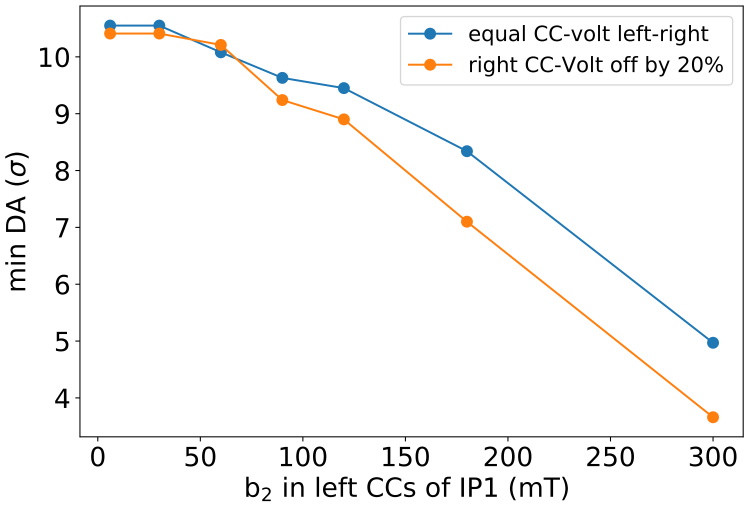

Figure 13: Minimum DA for 5 angles for different values of b_2 when the right hand side of the CC's has a quadrupolar component 20% more than the left side CC of IP1.

and the DQW models, no impact on the DA was observed for the case without misalignments, with 1 mm misalignment or when including beam-beam effects.

The multipolar components were then increased to observe at which point an impact is observed on the DA. Only two cases were observed when the DA was reduced: when increasing the quadrupolar multipole component to more than 30 mT on the DQW, or when increasing the sextupolar component to more than 20 times the nominal values on the DQW and RFD designs, but for this case the effect was only observed when 1 mm misalignments were considered in the CCs. When adding beam-beam effects the behaviour, and limits, were similar for the sextupolar case. For the quadrupolar component the impact on DA was observed until larger values (around 90 mT).

To analyse how mitigation of super-imposing effects in both IRs impact the DA, studies were done changing the sign between the components on both cavity designs for the two cases when an impact was observed (increasing quadrupolar or sextupolar components with misalignments). For the quadrupolar cases no units are present in the nominal RFD design; when a quadrupolar component is added, the decrease of DA with increasing quadrupolar values changed significantly, depending on the sign between CC models. When the sign between CC models is the same the limit remained the same than for the case without any quadrupolar components on RFD (around 30 mT), but the rate of decrease of DA for larger values of b_2 was much higher. When the sign between CC models is the opposite the limit increased to 60 mT, making this case even more stable than the one when quadrupole components are not present in the RFD model. Unlike the quadrupolar component, a sextupolar component is present in both models, although with opposite sign between them. Studies when both models have the same sign resulted in a much more stable DA, where the limit was met at 30 times the nominal values, to compare with the 20 times with the present (opposite) signs.

Both previous cases demonstrate that, when close to the limit, the signs between the models can make a big difference in terms of stability of the beam.

Studies were also done for octupolar and decapolar components, but DA remained unaffected for all cases (without misalignments, 1 mm misalignments and including beam-beam effects) even when increasing this value to up to 100 times the original ones. Therefore the previous limit set to be around 10^n for components of n-order can be relaxed as no evidence was found that the DA is affected on that region.

Acknowledgements

The authors of this work would like to thank the HL-LHC collaboration and UK-STFC. Special thanks also to R. Calaga and J. Mitchell for the updated values on the RF multipoles and R. Tomas and G. Arduini for fruitful discussions.

References

[1] J. Barranco, R. De Maria, A. Grudiev, R. Tomas, R.B. Appleby, and D.R. Brett. Long term dynamics of the High Luminosity Large Hadron Collider with crab cavities. *Phys. Rev. Accel. Beams*, 19:101003, 2016.

[2] P. Baudrenghien, K. Brodzinski, R. Calaga, O. Capatina, E. Jensen, A. Macpherson, E. Montesinos, and Parma V. Functional specifications of the LHC prototype crab cavity system. Technical report, CERN, February 2013.

[3] S. Verdu-Andres et al. Design and vertical tests of double-quarter wave cavity prototypes for the high-luminosity LHC crab cavity system. *Phys. Rev. Accel. Beams*, 21:082002, 2018.

[4] S.U. de Silva, H. Park, J.R. Delayen, Z. Li, and T.H. Nicol. Design and Prototyping of a 400 MHz RF-Dipole Crabbing Cavity for the LHC High-Luminosity Upgrade. In *Proceedings, 6th International Particle Accelerator Conference (IPAC 2015): Richmond, VA, USA*, page WEPWI036, 2015.

[5] Lattice repository:/afs/cern.ch/eng/lhc/optics/HLLHCV1.3.

[6] A. Latina and R. De Maria. RF multipole implementation. Technical report, CERN, October 2012.

[7] J. Mitchell. Private communication.

[8] R. Calaga and J. Mitchell. Latest info on field quality for crab cavities. Available at `https://indico.cern.ch/event/826475/contributions/3457534/attachments/1872608/3082026/WP2_Multipole_Update.pdf`, 2019.

[9] L. Deniau, H. Grote, G. Roy, F. Schmidt, and many other contributors. MADX. Available at `http://mad.web.cern.ch/mad/`.

[10] Sixtrack web site: `http://sixtrack.web.cern.ch/SixTrack/`.

[11] J. Barranco, R. Calaga, R. de Maria, M. Giovannozzi, A. Grudiev, and R. Tomás. Study of Multipolar RF Kicks from the main deflecting mode in Compact Crab Cavities for LHC. Technical Report CERN-ATS-2012-120, CERN, Geneva, May 2012.

5 Appendix

Table 3: Summary table of studies and recommended limits for CC multipoles studies in the HL-LHC. The columns indicate a summary of the study, whether misalignments (Mis.) or beam-beam effects are included (b-b), and the corresponding figure number. The limit is defined at the maximum value of the corresponding RF multipole for which no significant effect on DA is observed.

Fig.	**Study**	**Mis.**	**b-b**	**Limit**
1	Nominal values RF multipoles and hv crossing	N	N	Not found
1	Nominal values RF multipoles and vh crossing	N	N	Not found
2	Increasing quadrupolar component (b_2) in DQW. Nominal values for other RF multipoles	N	N	30 mT in DQW
3	Increasing quadrupolar component (b_2) in DQW. Nominal values for other RF multipoles	1 mm	N	30 mT in DQW
4	Increasing quadrupolar component (b_2) in DQW. Nominal values for other RF multipoles	N	Y	90 mT in DQW
5	Add b_2 units in RFD same sign. Nominal values for other RF multipoles	N	N	60 mT in DQW and RFD
5	Add b_2 units in RFD opposite sign. Nominal values for other RF multipoles	N	N	30 mT in DQW and -30 mT in RFD
6	Increasing b3 (in RFD) and a3 (in DQW) Nominal values for other RF multipoles.	N	N	100×b3(a3): 150,000 mT/m in DQW -50,000 mT/m in RFD
7	Increasing b3 (in RFD) and a3 (in DQW). Nominal values for other RF multipoles.	1 mm	N	20xb3(a3): 30,000 mT/m in DQW -10,000 mT/m in RFD
9	Increasing b3 (in RFD) and a3 (in DQW) [mT/m]	1 mm	Y	20xb3(a3): 30,000 mT/m in DQW -10,000 mT/m in RFD
10	Same (positive) sign in a3 in DQW and RFD [mT/m]	1 mm	N	30x b3(a3): 45,000 mT/m in DQW 15,000 mT/m in RFD
N/A	Increasing b4 and b5 in DQW and RFD	N	N	Not found
N/A	Increasing b4 and b5 in DQW and RFD	1mm	N	Not found
N/A	Increasing b4 and b5 in DQW and RFD	N	Y	Not found